Available online at www.sciencedirect.com
ScienceDirect
Journal of Nuclear Materials 367–370 (2007) 853–857
journal of nuclear materials
www.elsevier.com/locate/jnucmat

Effect of internal oxidation on the microstructure and mechanical properties of vanadium alloys

A.N. Tyumentsev [a,*], A.D. Korotaev [b], Yu.P. Pinzhin [a], S.V. Ovchinnikov [a], I.A. Ditenberg [a], A.K. Shikov [c], M.M. Potapenko [c], V.M. Chernov [c]

[a] *Institute of Strength Physics and Materials Science, SB RAS, 2/1 Akademichesky Avenue, Tomsk 634055, Russia*
[b] *Siberian Phisicotechnical Institute at Tomsk State University, 1 Novosobornaya Sq., Tomsk 634050, Russia*
[c] *A.A. Bochvar Research Institute of Inorganic Materials, 5 Rogov Street, Moscow 123060, Russia*

Abstract

This paper presents a short review of previous studies on the internal oxidation of vanadium alloys performed by the authors. These have investigated how internal oxidation affects the thermal stability of the microstructure of Zr-containing vanadium alloys and the temperature dependence of the short-term strength and plasticity characteristics of these alloys. Methods for producing highly dispersed heterophase materials stable up to temperatures close to the melting point have been substantiated. It has been shown that these methods efficiently increase the recrystallization temperature (up to $T \approx 0.8T_m$) for alloys subjected to internal oxidation in high-defect-density states. In combination with the high efficiency of precipitation hardening by ultrafine ZrO_2 particles, this provides a (1.5–2)-fold increase in short-term (including high-temperature, $T \leqslant 1100$ °C) strength of vanadium alloys while retaining good room temperature plasticity.

1. Introduction

A promising way of improving the thermal stability of the microstructure and high-temperature strength of metal alloys is to produce dispersed particles of carbide, nitride, or oxide phases, which are inert with respect to the matrix. Materials of this type can be produced by internal oxidation (IO) – the formation of oxide particles as a result of the selective oxidation of one or more alloy components during saturation with oxygen [1–3]. An attractive feature of this method is the possibility of forming highly dispersed two-phase structures, which are stable at temperatures close to the alloy melting point and provide a significant increase in recrystallization temperature (up to $T \sim 0.8T_m$, for vanadium $T_m = 1730$ °C). Moreover, the highly dispersed oxide particles and the high-angle and low-angle grain boundaries, being effective sinks for point defects, may substantially enhance the radiation resistance.

In this paper we summarize the results of investigations of the microstructure formation and mechanical properties of Zr-containing vanadium alloys subjected to IO and of the effect of chemo-thermal treatment (CTT) on the stability of the alloy microstructure. The investigations used 1-mm thick samples of V–0.45%Zr–0.2%C and

* Corresponding author.
E-mail address: tyuments@phys.tsu.ru (A.N. Tyumentsev).

0022-3115/$ - see front matter © 2007 Elsevier B.V. All rights reserved.
doi:10.1016/j.jnucmat.2007.03.070

V–5%Mo–0.9%Zr–0.3%C (at.%) alloys. The contents of hydrogen and nitrogen in the samples used were <0.005% and about 0.03%, respectively. The production, features of the initial (prior to IO) structure-phase state, the IO modes, and the experimental procedure are described elsewhere [4].

2. IO mechanisms for bcc alloys

It has been shown [3,4] that IO in the bcc alloys based on high-melting elements (V, Nb, and Ta) can occur by several mechanisms depending on the balance between the rate of formation of oxide particles and the rate of oxygen supply to the reaction zone. To analyze the conditions needed for a particular mechanism to occur, the kinetic parameter $K = C_O^s D_O / C_B D_B$ was introduced. Here C_O^s is the oxygen concentration at the sample surface, C_B is the concentration of the oxide-forming element in the alloy, and D_O and D_B are the respective diffusion constants of these elements. The numerator characterizes the rate of oxygen saturation and the denominator describes the rate of formation of oxides. For a depth of the reaction zone (or sample thickness) of about 1 mm, the following IO mechanisms are possible depending on the value of K [4]:

1. $K \ll 10^7$: IO develops as the two-phase region expands into the bulk of the sample and oxide particles precipitate at its boundary, which is called the internal oxidation front. As this takes place, the conditions for the nucleation and growth of particles of the second phase vary with distance from the surface in such a manner that the degree of dispersion of this phase decreases considerably as this distance increases, and highly dispersed two-phase structure can be produced only in a rather thin (tens of micrometers) surface layers. This is one of the basic disadvantages of the method, making it applicable only to workpieces of small thickness.
2. $10^7 \leqslant K \leqslant 10^{11}$: The diffusion of oxygen into the reaction zone occurs more rapidly than the formation of oxides, and the IO front transforms into a rather wide zone with dimensions comparable to the thickness of the sample. In this case, the oxide phase precipitates from supersaturated solid solutions, which are much more nonequilibrium than those inherent in the formation of the IO front. This provides an increase in density of particle nuclei (and, hence, in degree of particle dispersion) of the second phase and gives grounds to define this mechanism as the *nonequilibrium internal oxidation* mechanism [3,4]. Since the formation of oxide particles occurs simultaneously throughout the sample thickness, the thermodynamic and kinetic conditions of their nucleation and growth are almost independent of the distance from the surface and provide a uniform depth distribution of highly dispersed particles in the reaction zone.
3. $K \geqslant 10^{11}$: The IO can be subdivided into two stages: (1) low-temperature diffusion alloying with the formation, at a low diffusion mobility of the oxide-forming elements, of depth-homogeneous supersaturated solid solutions of these elements with oxygen and (2) precipitation of oxide particles during annealing at higher temperatures.

For bcc alloys, the kinetic parameter should increase on decreasing CTT temperature, because the temperature dependence of the diffusion of substitutional elements is much stronger than that of interstitial impurities (oxygen). In this case, the lowest IO temperatures correspond to the conditions most favorable for the formation of a highly dispersed, homogeneous oxide particle distribution throughout the thickness of the sample.

3. Features of formation of zirconium oxides in vanadium alloys during IO

For vanadium alloys of thickness 1 mm theoretical estimates [4] show that the temperature of rather rapid (within no more than several tens of hours) complete saturation of samples with oxygen, which is a decisive factor in judging the practical usability of the IO technology, is about 700 °C. For this case, for the mechanism of nonequilibrium IO the value of the kinetic parameter $K \sim 10^8$–10^{10} occurs in the temperature interval $T \sim 700$–900 °C.

These estimates were confirmed [4] by a comprehensive experiment performed to investigate the kinetics of redistribution of oxygen over the sample cross-section, the state of the solid solution, and the features of the two-phase structure at different IO stages using the electrical resistance measurement method, layer-by-layer measurement of microhardness, and electron microscopy. This is illustrated by the example of the V–5%Mo–0.9%Zr–0.3%C alloy. Samples of thickness 1 mm were annealed at 1350 ° C for 1 h, which lead to recrystallization of the samples and to complete dissolution of ZrC particles, and were then subjected to CTT in the

mode described in [4]. In this case, under the conditions of a low density of defects (consisting of dislocations and small-angle boundaries), the zirconium was completely in solid solution. The above theoretical estimates were obtained for such a structural state.

It has been shown that the IO of this alloy at $T = 750$–900 °C develops by the nonequilibrium mechanism. The oxidation reaction proceeds simultaneously throughout the thickness of the sample under thermodynamically nonequilibrium conditions of high supersaturation of the solid solutions of zirconium and oxygen in vanadium. Electron-microscopic examination has shown that under these conditions, the two-phase structure features a high degree of dispersion of the nonmetallic particles and only slight variation of this parameter with IO depth. In the surface layer of depth up to 400 μm, the particle diameters range from 3 to 8 nm, with average size about 5 nm (Fig. 1(a)). Larger particles (10–20 nm in diameter) are detected only in an interior layer greater than 400 μm from the surface (Fig. 1(b)).

4. Thermal stability of the microstructure of internally oxidized vanadium alloys

The thermal stability of the oxide phase formed upon IO is determined by the thermodynamic stability of this phase (the temperature intervals of its existence in the equilibrium state diagram) and by the rate of coarsening of the oxide particles.

According to [5], if a state diagram is not available, thermodynamic stability can be analyzed based on the thermodynamic potential of formation of second phases by the following relation:

$$(C_{\mathrm{Zr}}^{\mathrm{eq}}\gamma_{\mathrm{Zr}}) \times (C_{\mathrm{O}}^{\mathrm{eq}}\gamma_{\mathrm{O}})^2 \approx \exp(\Delta G^0_{\mathrm{ZrO_2}}/R_0T). \quad (1)$$

Here $C_{\mathrm{Zr}}^{\mathrm{eq}}$ and $C_{\mathrm{O}}^{\mathrm{eq}}$ are the values of the equilibrium solubility of zirconium and oxygen in vanadium; $\gamma_{\mathrm{Zr}} \sim 1$ and $\gamma_{\mathrm{O}} \approx \exp(\Delta G^0_{\mathrm{VO}}/R_0T)$ are the coefficients of activity of these elements; $\Delta G^0_{\mathrm{ZrO_2}}$ and ΔG^0_{VO} are the energy of formation of the respective oxides. With $\Delta G^0_{\mathrm{ZrO_2}} \approx -(1000$–$1100)$ kJ/mol and $\Delta G^0_{\mathrm{VO}} \approx -(360$–$400)$ kJ/mol we obtain $C_{\mathrm{Zr}}^{\mathrm{eq}}(C_{\mathrm{O}}^{\mathrm{eq}})^2 \approx 1.5 \times 10^{-10}$ and 7×10^{-8} for $T = 1000$ and 1700 °C, respectively. These low values of the solubility of zirconium oxide in vanadium result from this compound having a considerably higher value of the energy of formation than VO oxide and point to its high stability up to the melting point of vanadium ($T_{\mathrm{m}} = 1730$ °C).

It has been shown [4] that the growth of ZrO_2 particles in vanadium is controlled by the diffusion of zirconium atoms, and the rate of coarsening of these particles is determined by the expression

$$\mathrm{d}r^3/\mathrm{d}t = 8\sigma V^2 D_{\mathrm{Zr}} C_{\mathrm{Zr}}^{\mathrm{eq}}/9R_0T, \quad (2)$$

where r is the average radius of the particles, t is the time, σ is the energy of the particle–matrix interface, V is the molar volume of the oxide, and R_0 is the gas constant. In view of (1), this expression can be reduced to

$$\mathrm{d}r^3/\mathrm{d}t = \left[8\sigma V^2 D_{\mathrm{Zr}}\Big/9R_0T(C_{\mathrm{O}}^{\mathrm{eq}})^2\right] \exp\left[\Delta G^0_{\mathrm{ZrO_2}} - 2\Delta G^0_{\mathrm{VO}}\Big/R_0T\right]. \quad (3)$$

According to this expression, a decrease in rate of coarsening of the oxides and an increase in thermal stability of the highly dispersed two-phase structure should result from the increase in oxygen concentration in the solid solution of the internally oxidized samples.

This was confirmed experimentally by investigation of the thermal stability of the highly dispersed two-phase structure in all alloys examined. An example is the V–0.45%Zr–0.2%C alloy. The time

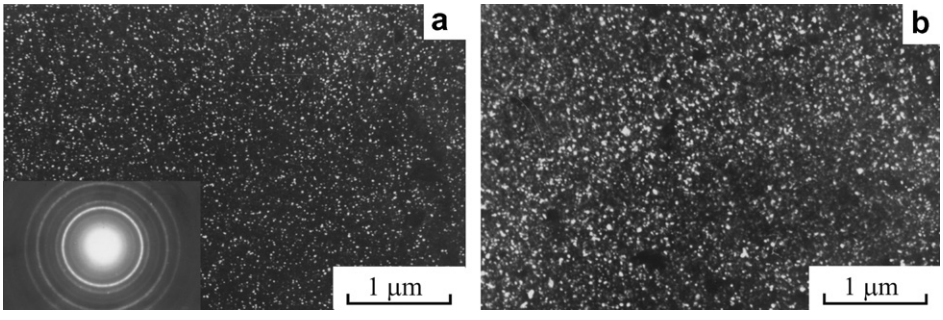

Fig. 1. Dark-field images of ZrO_2 particles in the V–0.45%Zr–0.2%C alloy after internal oxidation at 50 (a) and 500 (b) μm from the sample surface. $C_{[\mathrm{O}]} \approx 0.1$ at.%. These are replicas containing extracted second phase.

of IO for this alloy was varied to change the content of oxygen in solid solution that remained after the formation of ZrO_2 particles ($C_{[O]} \approx 0.1$, 0.3, and 0.5 at.%). Immediately after IO at $T = 750$–900 °C, the degree of dispersion of oxide particles (up to 10 nm in diameter with the most probable value $d \approx 5$ nm) is nearly the same as that presented in Fig. 1(a) and it does not depend on the treatment time. After annealing internally oxidized samples at $T = 1200$ °C for 1 h, these particles did not increase in size. Coarsening effects were detected only at temperatures of about $0.8T_m$. These effects are most pronounced for samples with the lowest concentration of oxygen in solid solution ($C_{[O]} \approx 0.1$ at.%). In these samples, annealing at 1350 °C for an hour, increased the particle size to $d \approx 50$–200 nm. As $C_{[O]}$ was increased to 0.3 at.%, the rate of coarsening decreased and the particle size after annealing was $d \approx 20$–50 nm. At the highest concentration of oxygen in the solid solution ($C_{[O]} \approx 0.5$ at.%), the rate of coarsening was a minimum and the particle size ranged between 10 and 25 nm.

A promising way of improving mechanical properties of bcc alloys is the formation of precipitates plus substructure hardening. This is one of a few methods of hardening with simultaneously increased plasticity of these alloys. Methods for this type of hardening by IO in high-defect-density states have been developed [4]. Examination of the thermal stability of the resulting structure has shown that the highly dispersed ZrO_2 particles, which are stable at $T \leqslant 0.8T_m$, efficiently stabilize the defect substructure, and this results in inhibition of recrystallization at these temperatures. For the V–5%Mo–0.9%Zr–0.3%C alloy, this is attained (Fig. 2) after IO with an excessive concentration of oxygen in the solid solution, $C_{[O]} \approx 0.7$ at.%.

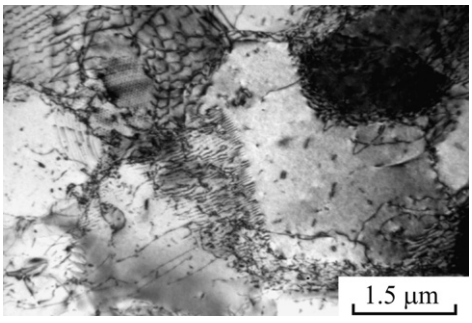

Fig. 2. Polygonization substructure in the V–5%Mo–0.9%Zr–0.3%C alloy after IO and subsequent annealing at 1300 °C for 1 h.

It seems likely that the highly dispersed oxide particles and the defect substructure, being effective sinks for radiation-produced point defects, enhance the radiation resistance of internally oxidized alloys. The oxygen in solid solution, needed for self-healing of a protective coatings based on thermodynamically stable oxide phases, is thus capable of providing the enhanced thermal stability of the coatings.

5. Effect of IO on mechanical properties of vanadium alloys

Investigations of the effect of IO on the temperature dependence of the yield stress, $\sigma_{0.1}$ of vanadium alloys (Fig. 3(a)) and on the features of the dislocation structure formed on deformation at different temperatures [4] have shown that the resulting highly dispersed oxide precipitates are not cut nor annihilated by moving dislocations down to the smallest particles ($d \approx 4$ nm). For room temperature, the precipitation hardening measurements are in good agreement with predictions based on the Orowan model [6]. The inverse particle size dependence of the degree of precipitation hardening ensures high precipitation hardening in alloys with ultrafine (a few nanometers) particles even at rather low volume content of the second phase.

Increasing deformation temperature reduces the effectiveness of precipitation hardening due to thermally activated creep of dislocations over the

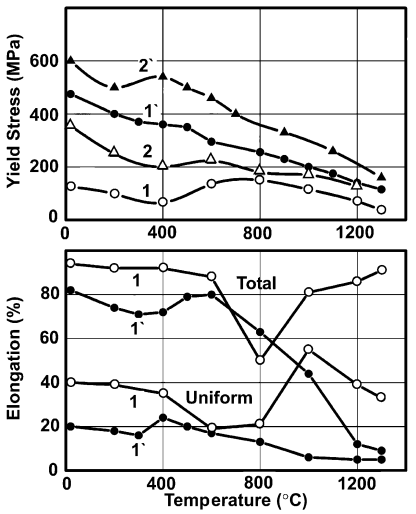

Fig. 3. Temperature dependences of the yield stress (top) and ductility (bottom) of the V–0.45%Zr–0.2%C (curves 1, 1′) and V–5%Mo–0.9%Zr–0.3%C (curves 2, 2′) after recrystallization at $T = 1350$ °C (1, 2) and subsequent IO (1′, 2′).

particles. Nevertheless, notwithstanding the rather strong temperature dependence of the yield stress, IO gives no less than a twofold increase in short-term strength, which is observed throughout the temperature interval investigated (from 20 to 1300 °C, see Fig. 3(a)). As can be seen from Fig. 3(b), this yield stress increase is achieved while high ductility of the alloys is retained.

6. Summary

The high solubility and diffusion mobility of oxygen at rather low ($T \leqslant 0.4T_m$) homologous temperatures, characteristic of vanadium alloys, allows nonequilibrium internal oxidation with formation of ZrO_2 particles simultaneously throughout the bulk of samples of thickness up to 1 mm under the conditions of high oxygen supersaturation of the V–Zr–O nonequilibrium solid solution. In this case, owing to a minor change in the conditions of nucleation and growth of the new phase on increasing the depth of internal oxidation, it is possible to produce a bulk-uniform distribution of ZrO_2 particles with a practically unlimited degree of dispersion (with particles a few nanometers in size).

The strongly negative formation energy of the ZrO_2 phase ensures high thermal stability of the finely dispersed two-phase structure and a strong dependence of the rate of coarsening of particles on the concentration of oxygen in the solid solution. Methods of internal oxidation with the formation of highly dispersed two-phase structures stable up to $T \approx 0.8T_m$ have been developed. For internal oxidation occurring in high-defect-density structures, these modes ensure inhibition of the recrystallization of internally oxidized alloys up to the above temperature.

These highly dispersed two-phase structures produced by internal oxidation of Zr-containing vanadium alloys and the high thermal stability of these structures result in a substantial increase in yield stress of these alloys over a wide temperature interval (from 20 to 1300 °C).

Acknowledgements

This work was supported in part by the Ministry of Education of the RF and CRDF (Project No. 016-02) and by RFBR (Grant Nos. 05-03-98003-r_ob_a and 05-08-50310-a).

References

[1] E.P. Danelija, V.M. Rozenberg, Internally Oxidized Alloys, Metallurgia, Moscow, 1978, p. 232 (in Russian).
[2] C.T. Liu, H. Inouye, R.W. Carpenter, Metall. Trans. 4 (1973) 1839.
[3] A.D. Korotaev, A.N. Tyumentsev, V.F. Sukhovarov, Dispersion Hardening of Refractory Metals, Nauka, Novosibirsk, 1989, p. 210 (in Russian).
[4] A.N. Tyumentsev, Yu.P. Pinzhin, S.V. Ovchinnikov, et al., Adv. Mater. 5 (2005) 5.
[5] E. Fromm, E. Gebhardt, Gases and Carbon in Metals, Metallurgia, Moscow, 1980, p. 712 (Russian translation).
[6] E. Orowan, Dislocations in Metals, AIME, New York, 1954, p. 131.